

¹ Bayesian inference of prehistoric population dynamics from multiple
² proxies: a case study from the North of the Swiss Alps

³ Martin Hinz^{1,2,*} Joe Roe¹ Julian Laabs³ Caroline Heitz³ Jan Kolář^{4,5}

⁴ 19 November, 2022

⁵ **Abstract**

Robust estimates of population are essential to the study of human–environment relations and socio-ecological dynamics in the past. Population size and density can directly inform reconstructions of prehistoric group size, social organisation, economic constraints, exchange, and political and social institutions. In this pilot study, we present an approach that we believe can be usefully transferred to other regions, as well as refined and extended to greatly advance our understanding of prehistoric demography. Here, we present a Bayesian hierarchical model that uses Poisson regression and state-space representation to produce absolute estimates of past population size and density. Using the area North of the main ridge of the Swiss Alps in prehistoric times (6000–1000 BCE) as a case study, we show that combining multiple proxies (site counts, radiocarbon dates, dendrochronological dates, and landscape openness) produces a more robust reconstruction of population dynamics than any single proxy alone. The model's estimates of the credibility of its prediction, and the relative weight it affords to individual proxies through time, give further insights into the relative reliability of the evidence currently available for paleodemographic research. Our prediction of population development of the case study area accords well with the current understanding in the wider literature, but provides a more precise and higher-resolution estimate that is less sensitive to spurious fluctuations in the proxy data than existing approaches, especially the popular summed probability distribution of radiocarbon dates. The archaeological record provides several potential proxies of human population dynamics, but individually they are inaccurate, biased, and sparse in their spatial and temporal coverage. Similarly, current methods for estimating past population dynamics are often simplistic: they work on limited spatial scales, tend to rely on a single proxy, and are rarely able to infer population size or density in absolute terms. In contemporary demography, it is becoming increasingly common to use Bayesian statistics to estimate population trends and project them into the future. The Bayesian approach is popular because it offers the possibility of combining heterogeneous data, and at the same time qualifying the uncertainty and credibility attached to forecasts. These same characteristics make it well-suited to applications to archaeological data in paleodemographic studies.

³⁰ ¹ Institute of Archaeological Sciences, University of Bern

³¹ ² Oeschger Centre for Climate Change Research, University of Bern

³² ³ CRC 1266 - Scales of Transformation, University of Kiel

³³ ⁴ Department of Vegetation Ecology, Institute of Botany of the Czech Academy of Sciences

³⁴ ⁵ Institute of Archaeology and Museology, Faculty of Arts, Masaryk University

³⁵ * Correspondence: Martin Hinz <martin.hinz@iaw.unibe.ch>

³⁶ Keywords: Prehistoric demography; Bayesian modelling; Multi-proxy; Settlement dynamics

³⁷ Highlights: - Bayesian modelling can integrate multiple, heterogeneous population proxies from the ar-
³⁸ chaeological record - Our initial model produces more robust, high-resolution estimates of past population
³⁹ dynamics than previous, single-proxy approaches - We provide absolute estimates of population size and
⁴⁰ density on the area north of the Swiss Alps in prehistoric times (6000–1000 BCE)

41 1. Introduction

42 Prehistorians have long recognised demography as a fundamental force in human cultural evolution (Childe,
43 1936). Despite decades of interest in the population dynamics of prehistoric societies, concrete estimates
44 of population size and density before written records remain elusive. Though the archaeological record
45 provides multiple possible demographic proxies (Müller and Diachenko, 2019), a lack of access to this data
46 and methodological tools for turning it into quantitative estimates has left the conclusions drawn from it
47 vague and superficial (Hassan, 1981). As a result, ‘expert estimates’ transferred from ethnographic parallels
48 have often taken the place of direct inference from archaeological evidence (Morris, 2013; Turchin et al.,
49 2015).

50 Prehistoric demography has experienced a resurgence in interest in recent years (Riede, 2009 and others in
51 same issue; Shennan, 2000), partly explained by a renewed interest in human–environment relations and
52 human impact, necessarily requiring an assessment of population size. Kintigh et al. (2014) list human influence,
53 dominance, population size, and population growth amongst their ‘grand challenges’ for archaeology
54 in the 21st century.

55 In particular, the ‘dates as data’ technique (Rick, 1987), using the frequency of radiocarbon dates as a proxy
56 for population dynamics, has been significantly developed in the last decade (e.g. Shennan et al., 2013) and
57 widely applied to archaeological contexts worldwide (Crema, 2022). This approach has contributed greatly
58 to our understanding of prehistoric demography, but is not without its critics (Attenbrow and Hiscock, 2015;
59 Carleton and Groucutt, 2021; Price et al., 2021). While the methodology continues to evolve and address
60 these critiques (Crema, 2022), it remains subject to fundamental problems common to all approaches relying
61 on a single proxy (French et al., 2021; Schmidt et al., 2021). We believe that these problems cannot be
62 overcome by methodological refinements in this area alone. Instead, a Bayesian approach offers a robust,
63 quantitative methodology for inferring prehistoric population dynamics from multiple proxies, including
64 summed radiocarbon dates.

65 Im Folgenden Artikel legen wir unsere Methodologie dar und zeigen seine Anwendung anhand eines Fall-
66 beispiels im Raum des Schweizer Mittellandes. Wir verwenden eine Art bayesisches Generalisiert Lineares
67 Modell (Kruschke, 2015), um die verschiedenen Proxies miteinander zu kombinieren, wobei ihre Bewertung
68 (Gewicht und Credibility Intervals) aus der Modellierung und der Kombination der Daten selbst hervorgeht
69 und nicht a priori festgesetzt ist. Weiterhin verfolgen wir das Konzept eines State Space Modells (Auger-
70 Méthé et al., 2021), a time series model in which the one time series is interpreted as the result of a noisy
71 observation of a stochastic process.

72 2. Background

73 2.1. Population estimation in prehistory

74 Proxies currently used for the estimation of population size in prehistory (following Müller and Diachenko,
75 2019) can roughly be divided into three groups: ethnographic analogies; deductive estimates from eco-
76 logical/economic factors; and the interpolation of frequencies of archaeological features (e.g. settlements,
77 structures, individual finds). Three basic problems are common to all these approaches:

- 78 1. **Reliance on single proxy:** Most investigations use only one source of evidence. Although multi-
79 proxy approaches exist, the individual proxies only serve to support each other or the main estimator,
80 without explicitly combining them.
- 81 2. **Uncertainty in measurements:** All archaeological evidence is inherently uncertain which is carried
82 through to derived measurements. However, in most studies, single curves are presented as estimates,
83 and the potential error associated is almost never specified.
- 84 3. **Lack of a transfer function:** By ‘transfer function’, we mean something that allows for the proxy data
85 to be interpreted in terms of actual population size or density. This could be absolute, i.e. a numerical

86 estimate of population, or relative, i.e. a means of scaling changes in the proxy value to changes in
87 population. Lack of suitable frameworks and ‘calibration’ data means that this is rarely presented
88 alongside proxy estimates. In the best cases, there is a qualitative assessment of the informative value
89 of the proxy, not sufficiently accounting for the complex nature of archaeological data.

90 Furthermore, the types of archaeological data commonly used as population proxies share a number of
91 problematic characteristics, being:

- 92 • **Limited:** We have only incomplete data, and it is usually not very informative.
- 93 • **Unevenly distributed:** For example, although there is a good data on settlement frequencies for
94 some regions, these regions are very unevenly distributed over time and space.
- 95 • **Noisy:** Frequently individual proxies are strongly influenced by factors unrelated to population, for
96 example taphonomic conditions or depositional biases.
- 97 • **Unreliable:** Research strategies, research history and varying levels of resources available to re-
98 searchers strongly affect the nature of compiled datasets. Systematic distortions are the rule rather
99 than the exception.
- 100 • **Heterogeneous:** All potential proxies have different spatio-temporal scales, granularity, information
101 value, scales, and data formats.
- 102 • **Indirect:** We will never have direct data on prehistoric population; only proxy data that is thought
103 to be a reasonable substitute. The transfer functions linking the proxy data with the desired quantity
104 (population) are unknown.
- 105 • **Contradictory:** When considering several proxies, differences in transfer functions, data quality and
106 noisiness inevitably lead to different results.

107 Many, if not all, of these problems can be ameliorated through a) the explicit, quantitative integration of
108 multiple proxies; and b) the use of a Bayesian approach to take account of and estimate uncertainty.

109 2.2. Hierarchical Bayesian demographic models

110 Many of the problems with archaeological population proxies are shared with contemporary demography. In
111 response, demographers have increasingly turned to Bayesian methods to estimate and forecast contemporary
112 population dynamics. For example, Bryant and Zhang (2018) consider Bayesian data modelling a solution
113 to exactly the kind of problems that affect archaeological data. Bayesian approaches are well suited for
114 limited, unreliable and noisy data. Various data sources, even contradictory data, can be brought into a
115 common framework and used to support one another. These methods also provide a quantitative estimate of
116 the likelihood and uncertainty of the model’s resulting predictions (or in our case retro-dictions). Bayesian
117 approaches are also capable of accounting for spatially and temporally incomplete data: where this data
118 is missing, the uncertainty increases, but this does not prevent general modelling and estimation. Finally,
119 hierarchically-structured model suites, with sub-models for each individual proxy, can be used to estimate
120 transfer functions between them and the value to be modelled, thanks to the interaction of a large number
121 of evidence.

122 This modeling technique can thus be used to join different lines of evidence horizontally and vertically and
123 combine their results into a overall estimate, including an assessment of their reliability: contradicting data
124 lead to a lower overall reliability, while a mutual support to smaller confidence intervals. If there is no
125 systematic bias that affects all data sources to the same extent, this results in the most reliable estimate
126 possible through the most heterogeneous set of data sources.

127 Bayesian radiocarbon calibration is a similar, well-established application in archaeology, where radiometric
128 uncertainty is modelled based on prior stratigraphic information. More recently, archaeologists have also
129 used Bayesian modelling techniques for testing hypotheses relating to demographic models based on ^{14}C data
130 (e.g. Crema and Shoda, 2021). This approach differs from the one presented here in that, in these analyses,
131 deductive models are generated and their plausibility is tested on the basis of ^{14}C data only. This is a clear

132 step forward to a model-based, scientific analysis. However, the use of only one proxy, exclusively for testing
133 hypotheses developed independently, creates problems comparable to those of the inductive approaches used
134 so far: lacking a combination with other indicators, one is limited to the problems and conditions of sum
135 calibration. Furthermore, this approach loses significant potential information that would be gained by a
136 direct evaluation of time series.

137 We attempt to make Bayesian hierarchical techniques usable for archaeological reconstructions. We want to
138 show, in a reproducible and practical form using a case study, how Bayesian methods can make a decisive
139 contribution to a better assessment of population development, crucial for the reconstruction of the human
140 past, even in for periods for which we only have very patchy, noisy and unreliable data.

141 **2.3. The Bayesian approach**

142 Bayesian statistics relies on the premise that there is always some prior assumption, even if very rough,
143 about the probability of an event. This assumption is adjusted by observing data, by checking how credible
144 these priors are (likelihood, see also Bryant and Zhang, 2018, p. 66). This is Bayesian updating (cf. also
145 Kruschke, 2015, especially 15–25), resulting in the posterior probability distribution, which represents not a
146 point prediction. Small amounts of data lead to a broad distribution not strongly localised and restricted.
147 Thus, we simultaneously obtained a result and an estimate the credibility interval, given the data.

148 This Bayesian learning is iterative and sequential, so that the result of one Bayesian inference can form the
149 prior of another (Kruschke, 2015, p. 17). This allows different information to be combined (Bryant and
150 Zhang, 2018, pp. 219–224), as it has long been exploited by archaeology in using stratigraphic information
151 to make radiometric dating more accurate (Ramsey, 1995).

152 This also makes a hierarchical formulation of problem domains possible. Parameters that are necessary for
153 an estimation, such as the relationship of population density to the deforestation signal in pollen data, need
154 not be specified explicitly, but can be given by probability distributions and then estimated in the model
155 itself (Bryant and Zhang, 2018, p. 186). The more data available, the more degrees of freedom can be
156 estimated with a reasonable width of credibility intervals (Kruschke, 2015, p. 112). For the estimation of
157 these parameters, submodels have to be created describing the relationship of the data to the characteristics
158 of the parameter (Kruschke, 2015, pp. 221–222).

159 **3. Materials: population proxy data**

160 Our case study area north of the Swiss Alps (Figure 1) covers about one third of Switzerland's territory and
161 comprises the partly flat, but largely hilly area between the Jura Mountains and the Alps. It is favourable
162 for settlement and agriculture; the Swiss Plateau between Lake Zurich and Lake Geneva is by far the most
163 densely populated region of the Switzerland today. This serves as our core region of interest because it
164 is here that archaeological data is most abundant and accessible. The region has a very diverse natural
165 landscape: shaped by glaciers during the ice ages, the many lakes and bogs provide excellent preservation
166 conditions for the numerous Neolithic and Bronze Age lakeside settlements, and a rich source for vegetation
167 reconstructions by means of pollen analyses. Thanks to very active and efficient archaeological research and
168 heritage management there is an abundance of archaeological information, including known sites as well as
169 dendrochronological and ^{14}C data.

170 Our case study targets the period between 6000–1000 BCE. The lower limit of this time window was chosen
171 to avoid the so-called 'Hallstatt plateau' in the Northern Hemisphere radiocarbon calibration curve, which
172 causes difficulties for the ^{14}C proxy. The upper limit coincides with post-glacial changes in pollen spectra,
173 before which the openness indicator is highly unlikely to reflect human influence.

174 A large number of different proxies can be integrated into a model of this type, provided that these ob-
175 servations a) can be understood as dependent on the population density in the past, and b) a model-like
176 description of this dependence can be created. Table 1 provides a non-exhaustive list. For our case study,

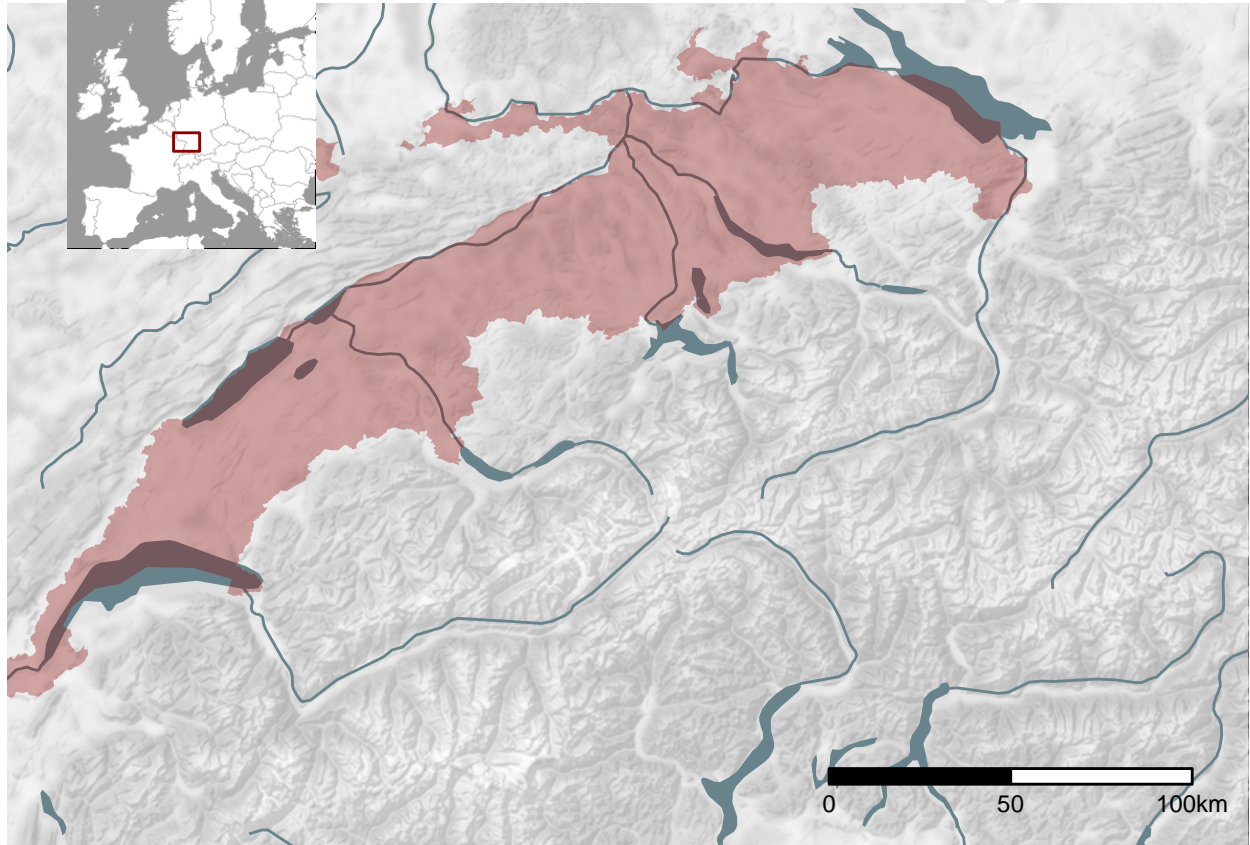


Figure 1: Location and extent of the Swiss Plateau as biogeographical region (based on swisstopo) including additional low altitude areas in the north of Switzerland (regions along the High Rhine between Schaffhausen and Basel).

¹⁷⁷ we used a landscape openness indicator; an aoristic sum of typological dated sites; a sum calibration; and
¹⁷⁸ frequency data for dendro-dated lakeshore settlements in the Three Lakes region (western Swiss Plateau).

Table 1: An incomplete list of possible observation that can be linked to population developments in the past. Proxies used in this study are highlighted.

Proxies
Expert estimates
Ethnographic Analogies
Carrying Capacity
Economic modelling
Extrapolation of buried individuals
Burial anthropology
Settlement data, number of houses
Settlement data, settlement size
Aoristic analysis
Dendro dates
Amount of archaeological objects
Radiocarbon sum calibration
Estimates based on specific object types
Human impact from pollen or colluvial data
aDNA based estimates
...

¹⁷⁹ 3.1. Dendro-dated lakeshore settlements

¹⁸⁰ From the Neolithic onwards, known settlement areas in Switzerland concentrate along its rivers and lakes
¹⁸¹ (Christian Lüthi, 2009). Thus, our working region offers excellent data for demographic estimation, but
¹⁸² poses very specific problems for such an undertaking. We have high-resolution information on the temporal
¹⁸³ sequence of individual lakeside settlements by means of dendro data. In these cases, ¹⁴C data are not as
¹⁸⁴ abundant simply because they are inferior to dendro dating.

¹⁸⁵ The dataset we use for the number of dendro-dated wetland settlements in the Three Lakes region was
¹⁸⁶ collected by Julian Laabs for his PhD thesis (Laabs, 2019). The time series used here runs from 3900 to 800
¹⁸⁷ BCE, and contains the number of chronologically registered fell phases at individual settlements.

¹⁸⁸ 3.2. Summed radiocarbon

¹⁸⁹ The dataset for the ¹⁴C sum calibration primarily consists of data from the XRONOS database (<https://xronos.ch>), supplemented by dates from the unpublished PhD thesis of Julian Laabs (Laabs, 2019) and
¹⁹⁰ the data collection of Martínez-Grau et al. (2021). It contains a total of 1135 single ¹⁴C data from 246 sites
¹⁹¹ (see Figure 2). The dates in the dataset range in ¹⁴C years from 10730 to 235 uncal BP. This time window
¹⁹² extends beyond the study horizon in order to minimise boundary effects.

¹⁹⁴ We binned the data at site levels to obtain a temporally dispersed count and thus an expected value of
¹⁹⁵ contemporaneous ¹⁴C dated sites. For the creation of the sum calibration, the corresponding functions of
¹⁹⁶ the R package rcarbon (Crema and Bevan, 2021) were used with their default settings.

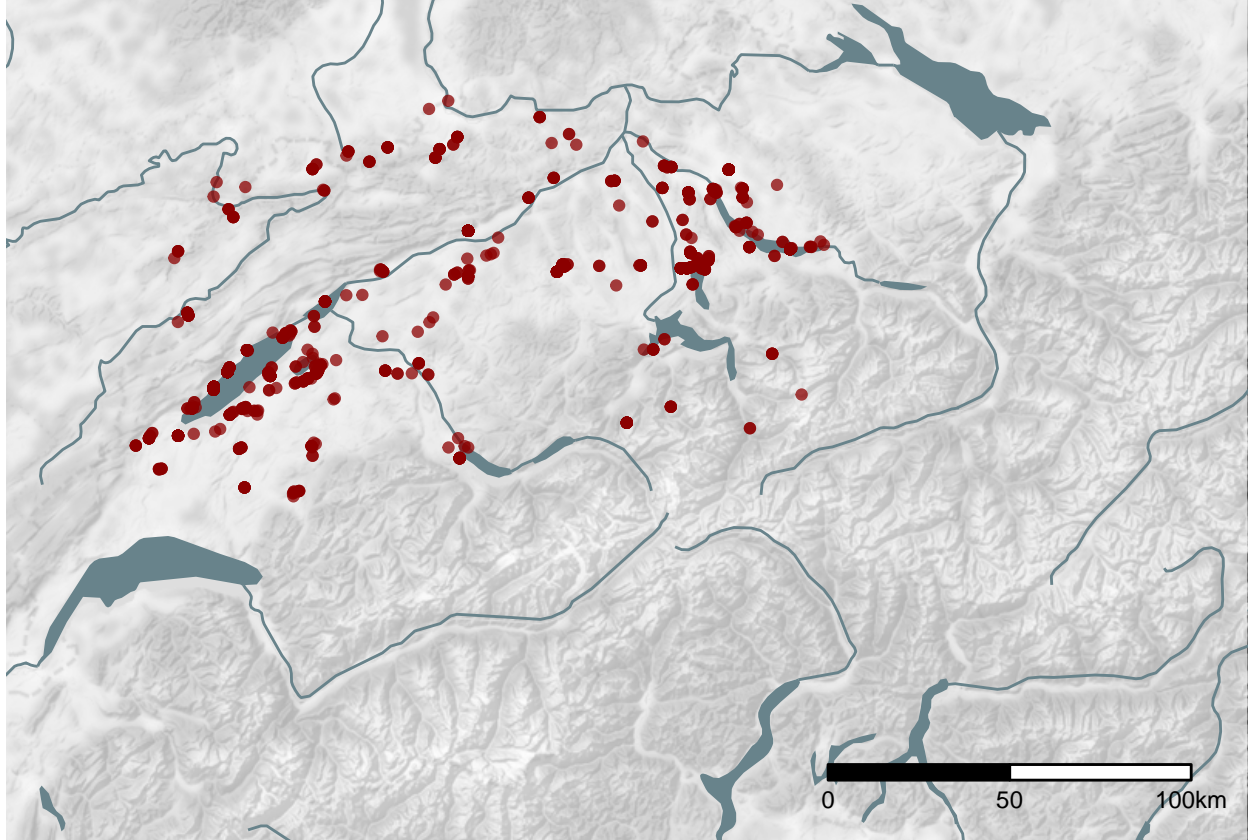


Figure 2: The location of the ^{14}C dated sites in the dataset.

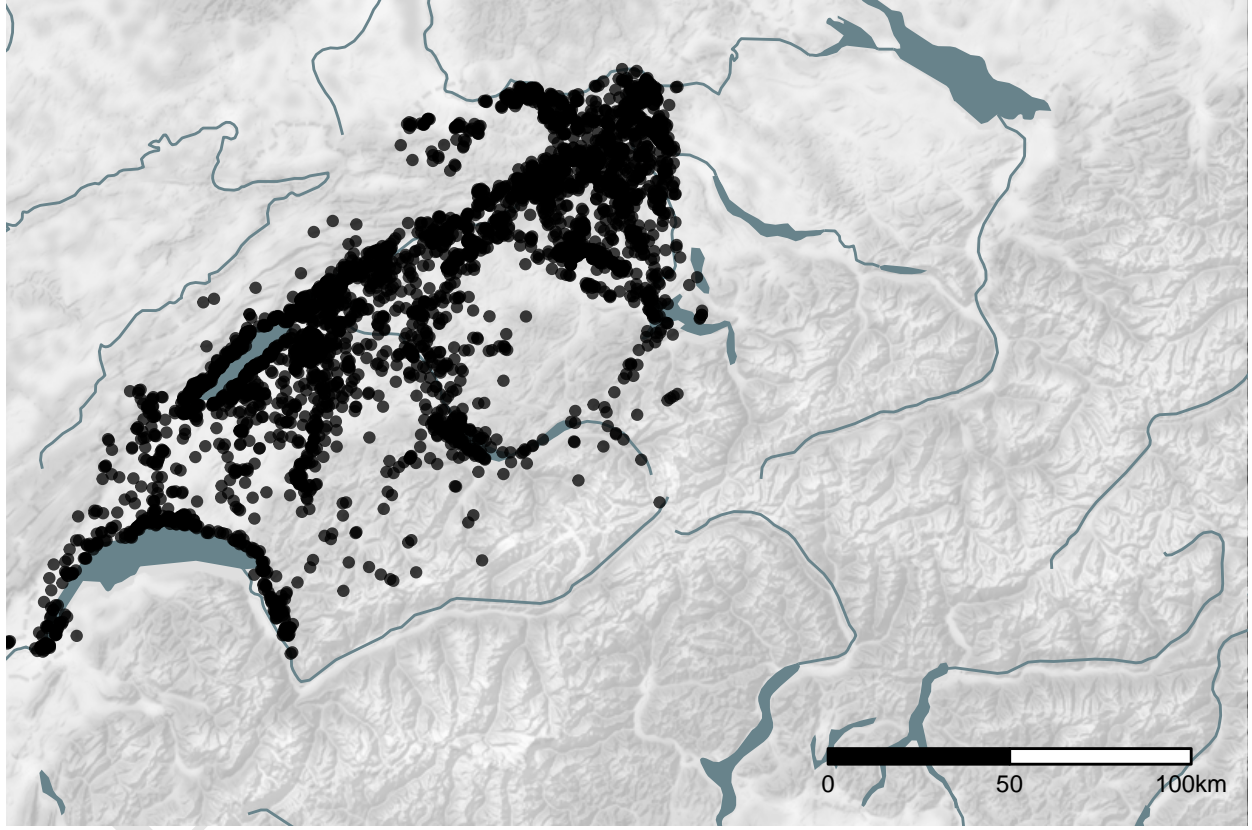


Figure 3: Location of the sites from the find reports of cantonal archaeology (heritage management) authorities. Locations are ‘fuzzed’ by approximately 1 km.

¹⁹⁷ 3.3. Aoristic sum

¹⁹⁸ We include relative dating information obtained from the heritage authorities of the Swiss cantons (Figure
¹⁹⁹ 3). These are primarily derived from scattered surface finds, often with a low dating accuracy (only in the
²⁰⁰ range of archaeological periods), incorporated into our model as a typologically-dated, aorist time series.
²⁰¹ However, it is not dependent on radiocarbon dating and thus it avoids the methodological issues of sum
²⁰² calibration. Data from 4321 sites were included in the aoristic sum.

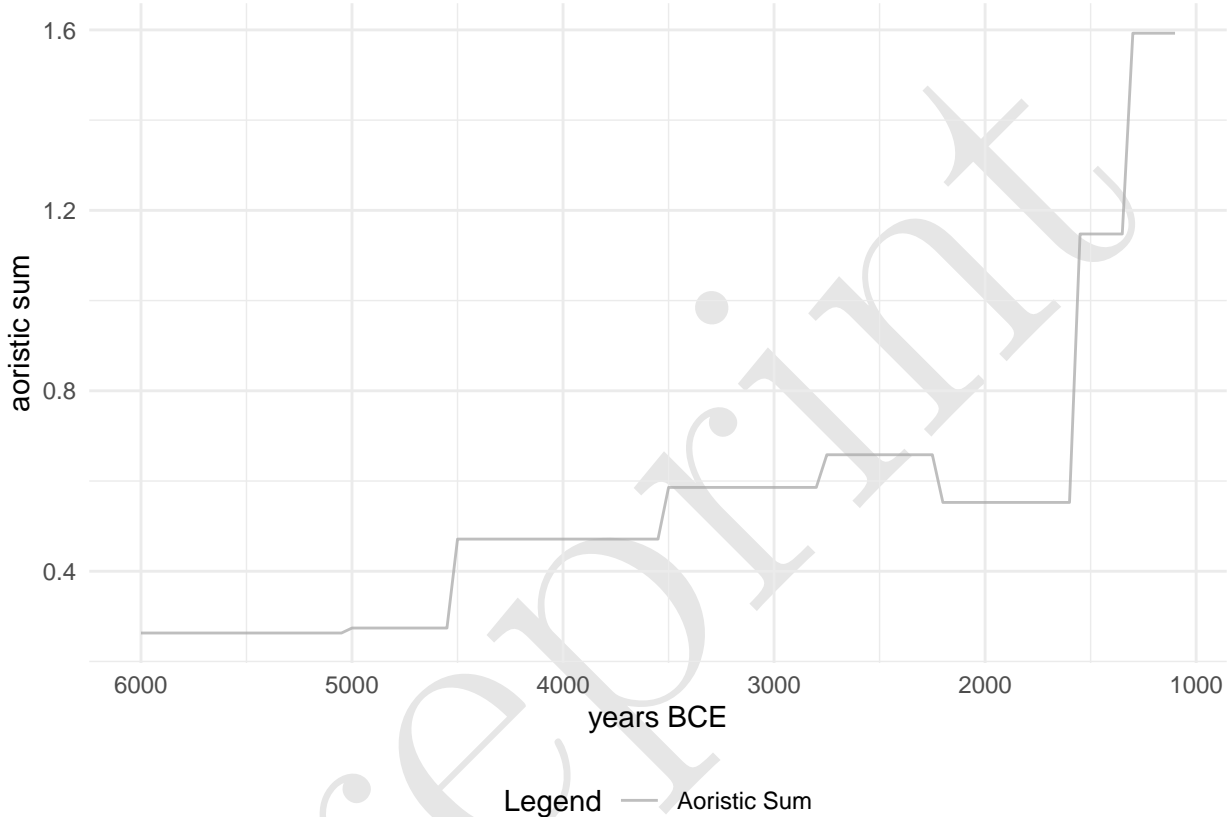


Figure 4: Aoristic sum of archaeological sites used in the analysis.

²⁰³ 3.4. Landscape openness

²⁰⁴ Natural conditions in the Swiss lakes enable not only highly precise dating of archaeological sites, but also
²⁰⁵ a very dense network of pollen analysis. We make use of this by generating a supra-regional openness
²⁰⁶ indicator for the vegetation from the pollen data (Figure 5). This proxy has the specific advantage that it is
²⁰⁷ not dependent on archaeological preservation conditions, making it particularly valuable for compensating
²⁰⁸ systematic distortions that result from archaeological taphonomy and period-specific settlement patterns.

²⁰⁹ We assume that the higher the population density in an area, the greater the human influence on the natural
²¹⁰ environment (Lechterbeck et al., 2014; Zimmermann, 2004). Evidence of deforestation can therefore provide
²¹¹ indications of population dynamics. The full procedure for deriving this proxy from several different pollen
²¹² diagrams is detailed in a previous publication (Heitz et al., 2021). Here, we use five pollen diagrams from
²¹³ sites mainly in the hinterland of the large Alpine lakes.

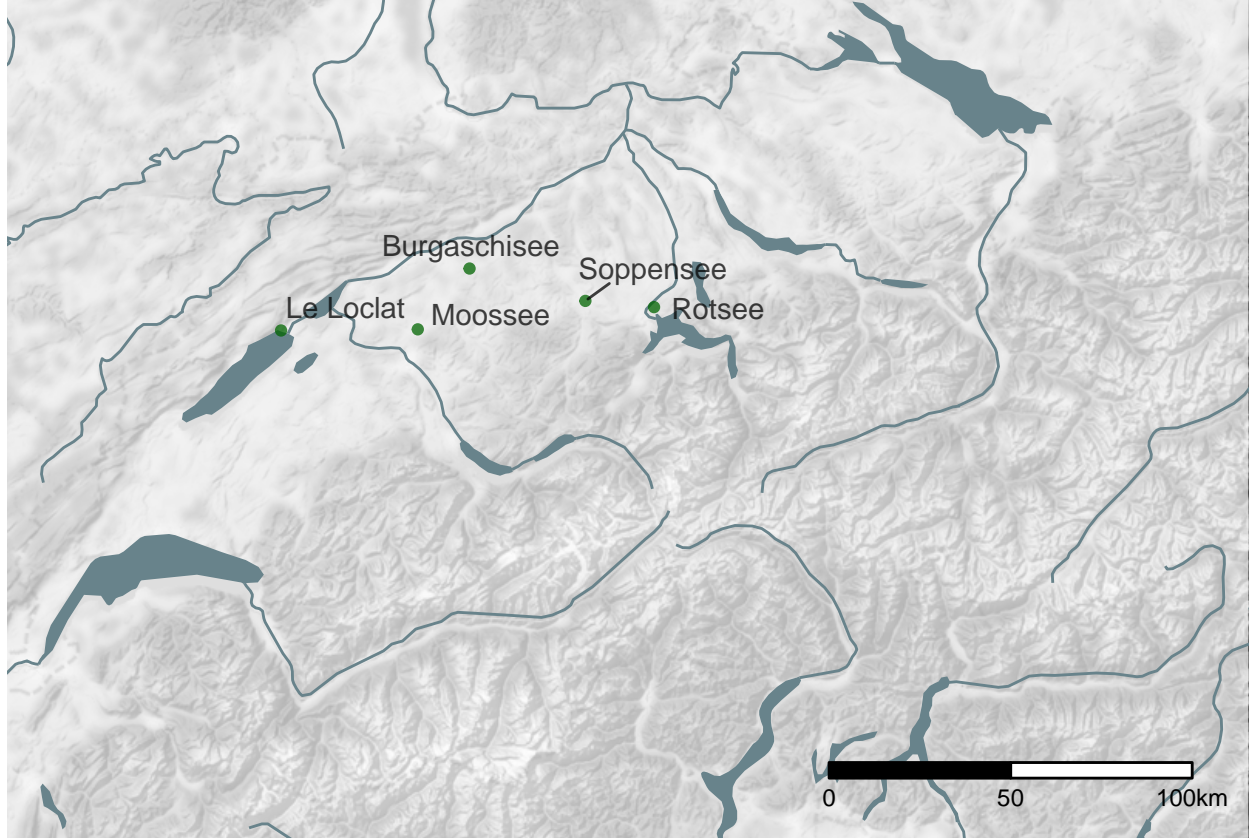


Figure 5: Location of the pollen profiles used for the openness indicator.

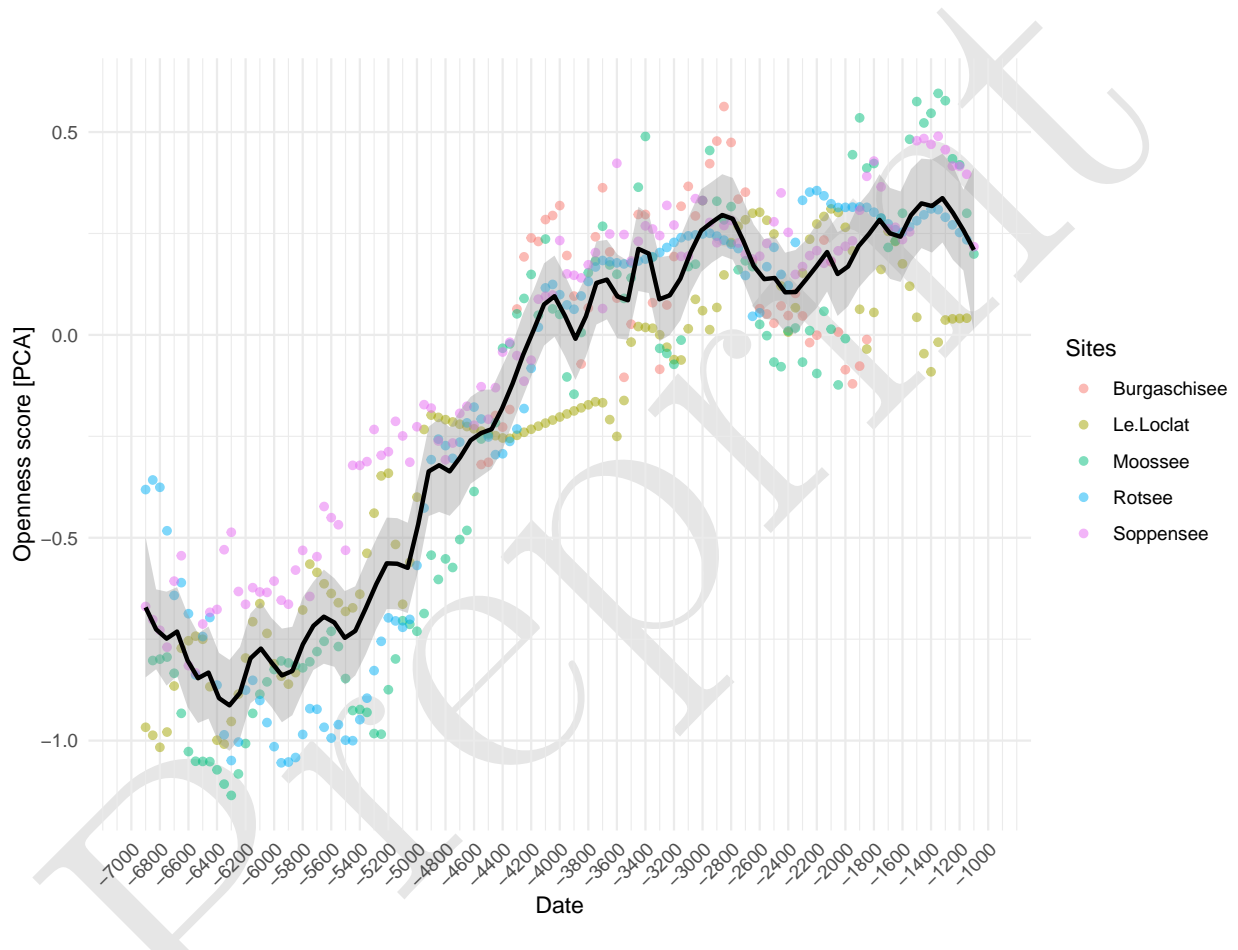


Figure 6: Value on the first dimension of the PCA against dating of the samples for the individual pollen profiles and their combined average value as the openness indicator.

²¹⁴ **4. Methods: Bayesian model**

²¹⁵ Sum calibration, openness and the dendro-dated settlement data was smoothed by a moving average with
²¹⁶ a 50 years window, corresponding to the unified sampling interval for all proxies. The aoristic sum was not
²¹⁷ smoothed, because it already has a very coarse temporal resolution. In the construction of our ‘observational
²¹⁸ model’, we considered all these proxies as informative of the number of settlements located in the north of
²¹⁹ the Swiss Alps. Population development is simulated in a ‘process model’ using a Poisson process.

²²⁰ **4.1. Process model**

²²¹ A special class of Bayesian hierarchical models are so-called ‘state space models’, specifically designed for
²²² time series. They follow two principles. First, a hidden or latent process is assumed, representing the state
²²³ of the variable of interest x_t through the entire time series. Every state of variable x in the future, as well
²²⁴ as in the past, is bound by a Markov process to the state of variable x at time t . Second, it is assumed
²²⁵ that certain observations, represented in variable y , are dependent on the state of variable x at time t . This
²²⁶ implies that a relationship between the individual states of variable y is generated over time via the hidden
²²⁷ variable x , which is not directly observable.

²²⁸ This structure makes these models particularly suitable for demographic reconstruction using archaeological
²²⁹ and other data. Population density itself is not directly measurable: all we have at our disposal are
²³⁰ observations derived by unknown transfer functions.

²³¹ Our overall model is broken down into several hierarchically-connected individual elements. The process
²³² model represents the demographic development itself, without already being explicitly parameterised with
²³³ data. Here we assume that the latent variable ‘number of sites’ is strongly autocorrelated across different
²³⁴ time periods. The number of sites in 3000 BCE is strongly conditioned by the number of sites in 3050 BCE,
²³⁵ and so on. The population at time t results from the population at time $t - 1$ times a parameter λ , which
²³⁶ represents the population change at this time.

$$N_t = N_{t-1} * \lambda_t$$

²³⁷ A univariate discrete Poisson distribution is particularly suitable for modelling frequencies, numbers of events
²³⁸ that occur independently of each other at a constant mean rate in a fixed time interval or spatial area. It is
²³⁹ determined by a real parameter $\lambda > 0$, describing the expected value and the variance. Thus, the relationship
²⁴⁰ shown above can be rearranged as follows:

$$\begin{aligned} N_t &\sim dpois(\lambda_t) \\ \lambda_t &= N_t \end{aligned}$$

²⁴¹ If we now have information about the change in population development (the proxies), this can enter into the
²⁴² model via a change in λ in form of a regression: for all proxy values — represented as a vector of independent
²⁴³ variables $x \in R^n$, with R^n as an n-dimensional Euclidean space defined by the n variables — the model
²⁴⁴ takes the form:

$$\log(E(Y | x)) = \alpha + \beta'x$$

²⁴⁵ Using the logarithm as a link function ensures that λ , which must always be positive, can also be described
²⁴⁶ by variables that may also be negative. β serves as slope factor, as in a normal linear regression. Here, it
²⁴⁷ functions as a scaling factor for the individual proxies. α is to be understood as an intercept, representing
²⁴⁸ a baseline when there were no change due to the variables. This is the desired behaviour: λ is equal to the
²⁴⁹ value of the population in the previous time period, plus or minus the changes resulting from the variables.

$$\log(\lambda_t) = \log(N_{t-1}) + \sum_{i=1}^n \beta_i x_{t,i}$$

250 Since λ and N are essentially in the same range (e.g. if $lambda = 1$, the expected value for N would also be 1),
 251 N_{t-1} must also be log-transformed for the congruence of both values. Population size N_t as well as population
 252 change λ_t are time-dependent. At each individual point in time, these variables will take on different values.
 253 But we can assume that the population change will not exceed certain limits (*max_change_rate*), though
 254 it is not possible to specify this at this point.

$$\begin{aligned} max_growth_rate &\sim dgamma(shape = 5, scale = 0.05) \\ N_t/N_{t-1} &< (max_growth_rate + 1) \\ N_{t-1}/N_t &< (max_growth_rate + 1) \end{aligned}$$

255 A gamma distribution centres probability in the range $[0, 1]$; adding 1 makes this range $[1 - 2]$. This prevents
 256 the number of sites from explosively increasing between two time periods, which would lead to problems for
 257 the convergence of the model. The estimation of this parameter for the entire model, as well as the estimation
 258 of the respective population change per time section, results from the modelling and the interaction with
 259 the data.

260 4.2. Observational model

261 In this initial implementation, the observational model is essentially a Poisson regression, where the proxies
 262 are used to inform the change in the number of settlements between time steps. The individual proxies were
 263 z-normalised and absolute differences between time steps were then computed. If the value of the proxy
 264 increases, this results in a positive difference from the previous time step, and vice versa.

$$\begin{aligned} z_t &= \frac{x_t - \bar{x}}{\sigma_x} \mid \sigma_x := Standard\ Deviation \\ \delta z_t &= z_t - z_{t-1} \end{aligned}$$

265 The sum of the resulting differences between the time steps, together with the settlement number of the
 266 previous step as the expected value, then forms λ_t : the expected value for the settlement number of the
 267 current time step.

$$\log(\lambda_t) = \log(N_{t-1}) + \sum_{i=1}^n \beta_i \delta z_{i,t}$$

268 Here, β_i is a scaling factor that represents the influence of the respective proxy. It is a confidence value of
 269 the model for the respective proxy, so that the sum of all β_i results in 1.

$$\sum_{i=1}^n \beta_i = 1$$

270 A Dirichlet distribution—a multivariate generalization of the beta distribution—is commonly used for this
 271 purpose in hierarchical Bayesian modelling. Its density function gives the probabilities of i different exclusive
 272 events. It has a parameter vector $\alpha = (\alpha_1, \dots, \alpha_n) \mid (\alpha_1, \dots, \alpha_n) > 0$, for which we have chosen a weakly infor-
 273 mative log-normal prior. The priors for the log-normal distribution in turn come from a weakly informative
 274 exponential distribution for the mean and a log-normal distribution with μ of 1 and σ_{log} of 0.1:

$$\begin{aligned}
\beta_i &\sim Dir(\alpha_{1-i}) \\
\alpha_i &\sim LogNormal(\mu_{alpha_i}, \sigma_{alpha_i}) \\
\mu_{alpha_i} &\sim Exp(1) \\
\sigma_{alpha_i} &\sim LogNormal(1, 0.1)
\end{aligned}$$

275 Intuitively, we consider the sum of the proxies as determinant of the number of settlements. That is, the
276 share of each individual proxy is variable and is estimated within the model. This share is recorded within
277 the model as the parameter p.

278 The error value is represented by the Poisson process in the process model. In this implementation, the
279 model finds the best possible combination between the individual proxies to describe a settlement dynamic.
280 The number of sites is converted into population density using (certainly debatable) parameters defined by
281 us, but which are only scaling factors for the intermediate value of number of settlements. We assume that
282 each site represents a number of people that is poisson distributed around the value 50, a compromise, as
283 both Mesolithic and Neolithic and Bronze Age settlement communities need to be represented. An evidence-
284 based estimate data series of the temporal development of settlement sizes could enhance this specification.
285 From the number of sites and the mean number of individuals a population density can be calculated using
286 the case study area (12649 km^2), making the models estimate comparable with estimates from other sources
287 or the literature.

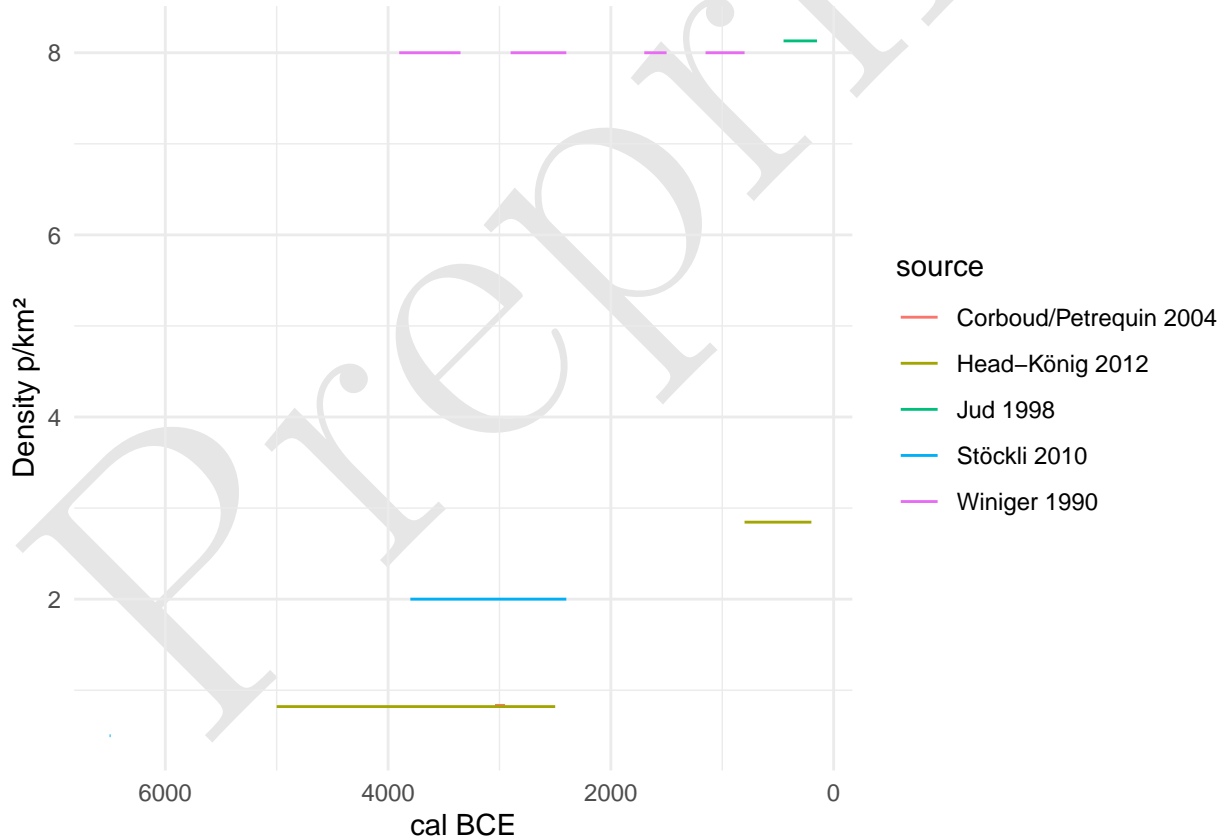


Figure 7: Expert estimate of population density on the Swiss Plateau.

288 **4.3. Model fitting**

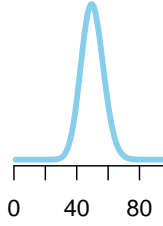
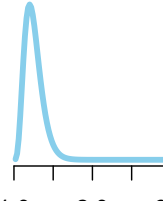
289 The model was fitted using the R package *nimble* (version 0.11.1, R version 4.1.3), using 4 parallel chains.
290 Achieving and ensuring convergence and sufficient effective samples (10000) for a reliable assessment of the
291 highest posterior density interval was carried out in steps.

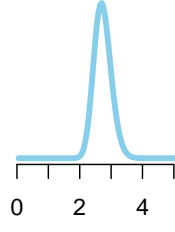
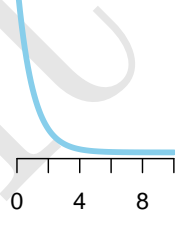
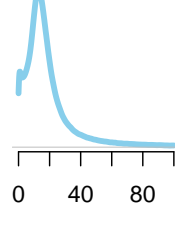
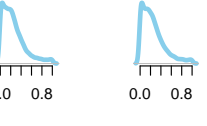
- 292 1) the model was initialised for each chain and run for 100000 iterations (with a thinning of 10). On
293 a reasonably capable computer (Linux, Intel(R) Xeon(R) CPU E3-1240 v5 @ 3.50GHz, 4 cores, 8
294 threads), this takes approximately a minute.
- 295 2) the run was extended until convergence could be determined using Gelman and Rubin's convergence
296 diagnostic, the criterion being that a potential scale reduction factor of less than 1.1 was achieved for
297 all monitored variables. Convergence occurred after about thirty seconds.
- 298 3) Due to the high correlation of the parameters and thus a low sampling efficiency, the collection of at
299 least 10,000 effective samples for all parameters took about five hours.

300 A starting value of 5 p/km² for the population density of the Late Bronze Age (1000 BCE) was taken from
301 the literature, which may represent a general average value for all prehistoric population estimates (Nikulka,
302 2016, p. 258). For the model, this was set as the mean of a normal distribution with a standard deviation of
303 0.5, which should give enough leeway for deviations resulting from the data. Nevertheless, it should be noted
304 that our resulting estimate is strongly conditioned by this predefined value, especially in the later sections.

305 For traceplots and the prior-posterior overlap, as well as density functions of the posterior samples of the
306 individual parameters, please refer to the supplementary material.

Table 2: Priors and fixed parameters used in the model.

Priors	Value	Plot/Comment
MeanSiteSize	dpois(50)	
max_growth_rate	dgamma(shape = 5, scale=0.05) + 1	

Priors	Value	Plot/Comment
mu_alpha	dlnorm(1,sdlog=0.1)	
a_alpha	dexp(1)	
alpha	dlnorm(mu_alpha[j],sdlog=a_alpha[j])	
p	ddirch(alpha[1:4])	
Parameters		
nEnd	5	
AreaSwissPlateau	12649 km ²	
Initial Values		
lambda _{1:nYears}	$\log(1 - 10^{\frac{1}{nYears-1}})$	exponential increase of the factor 10
PopDens _{1:nYears}	nEnd (=5)	
nSites _{1:nYears}	50	

307 **5. Results**

308 The population density estimated by the model (Figure 8) ranges between 0.2 p/km² for the beginning (6000
 309 BCE) and 4.8 p/km² for the end of the estimate (1000 BCE), reaching a maximum of 6.5 p/km² for around
 310 1250 BCE. This remains within the range considered plausible according to expert estimates. There are

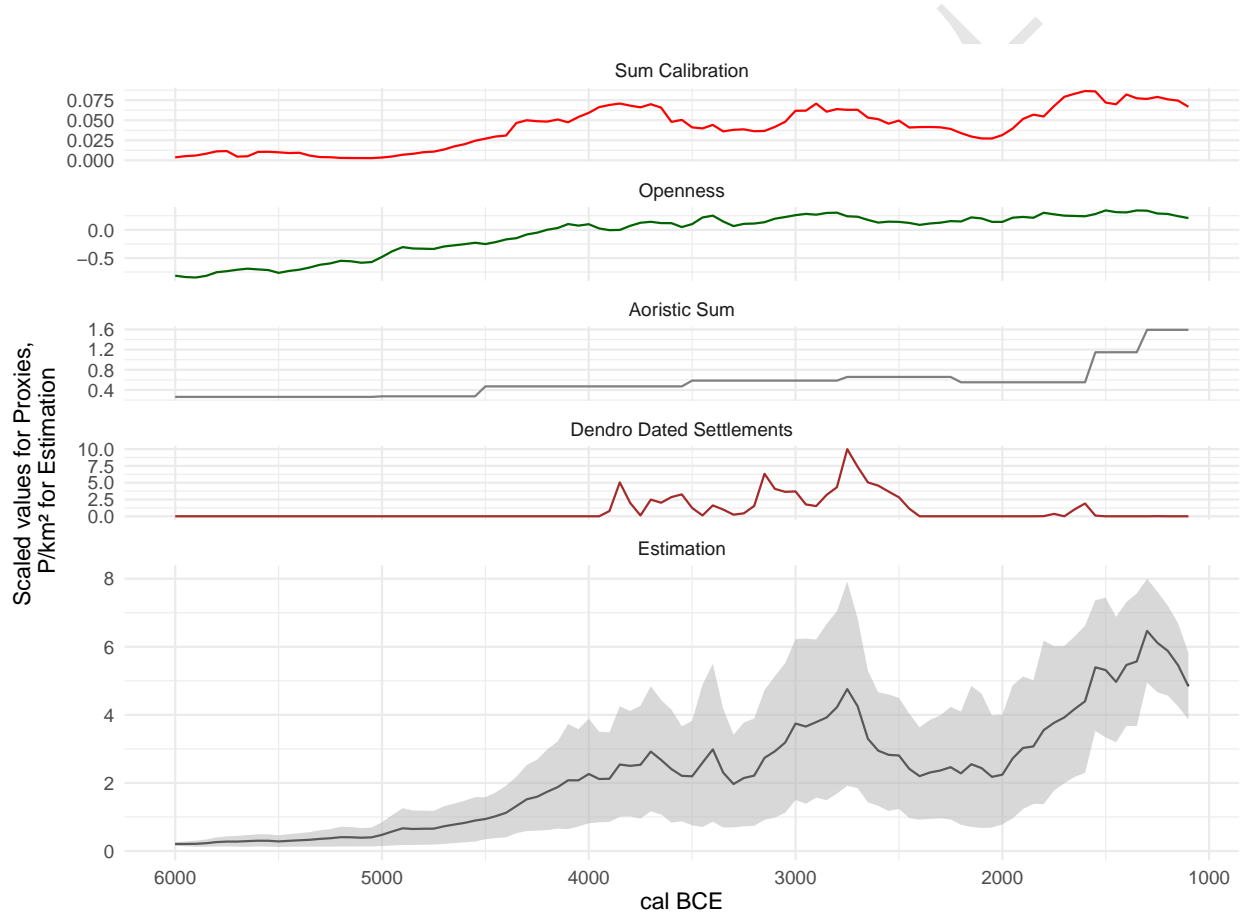


Figure 8: Estimate of population density predicted by the model. The four input proxies are also plotted (scaled) for comparison.

311 clear peaks around 1250 BCE and around 2750 BCE, which corresponds to the beginning of the influence of
 312 Corded Ware ceramic styles (Hafner, 2004).

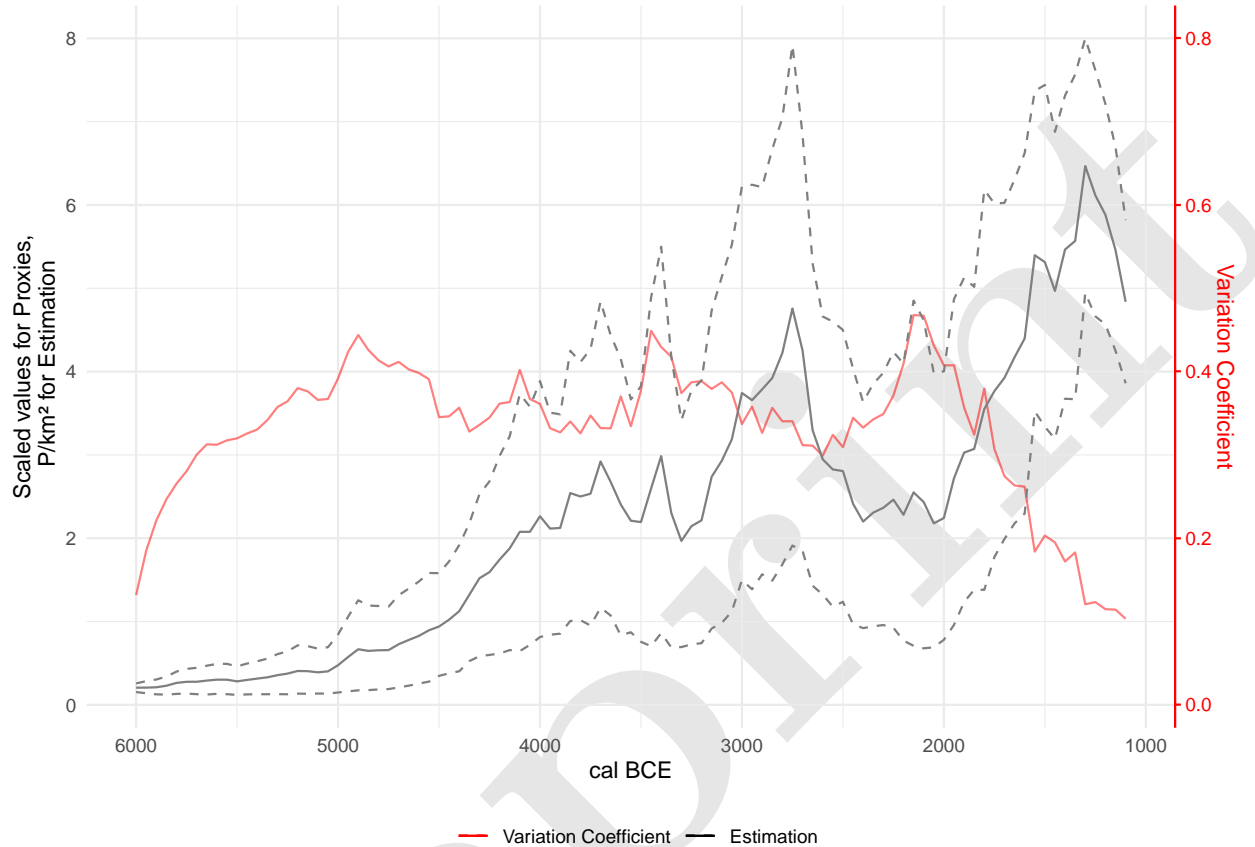


Figure 9: Variability of the model estimate of population density over time, with the estimate itself for reference.

313 The temporal distribution of variability in the estimate (Figure 9) allows us assess at which time steps the
 314 uncertainty is greater due to e.g. contradictions in the proxies. The coefficient of variation is 0.13 for the
 315 beginning and 0.1 for the end of the estimate, with the greatest variability (0.47) seen around 2150 BCE.
 316 This is not surprising as there are fewer archaeological contexts recorded from the earlier phase of the Early
 317 Bronze Age, c. 2200-1800 BCE. This picture changes from c. 1800 BCE onwards (David-Elbiali, 2000; Hafner,
 318 1995). The beginning and end of the time series are relatively clearly determined, resulting from the *a priori*
 319 setting of final population density, but also from the uniformity of the proxies during these periods. Overall,
 320 the variability is relatively stable over the entire estimation and averages 33% of the respective mean.

321 The parameter p reflects the relative weight given to the individual proxies. Its posterior distribution (Figure
 322 10) shows that the model weights the openness indicator the highest, averaging slightly above 60%, followed
 323 by the sum calibration, with an average of about 20%. The aoristic sum is slightly above 10%, whereas the
 324 importance of the dendro-dated settlements is below 10%. The reason for the latter is certainly that there
 325 are no lakeshore settlements over large areas of the time window, and therefore the overall confidence in the
 326 proxy is low. The aoristic sum is flat for long periods, making it difficult to integrate with other proxies.
 327 The sum calibration shows very strong short-term fluctuations, at least partly due to the calibration curve,
 328 which suggests that it does not reliably represent a continuous population trend. Its fluctuations have an
 329 impact on the model's estimate, albeit to a lesser extent than the general trend.

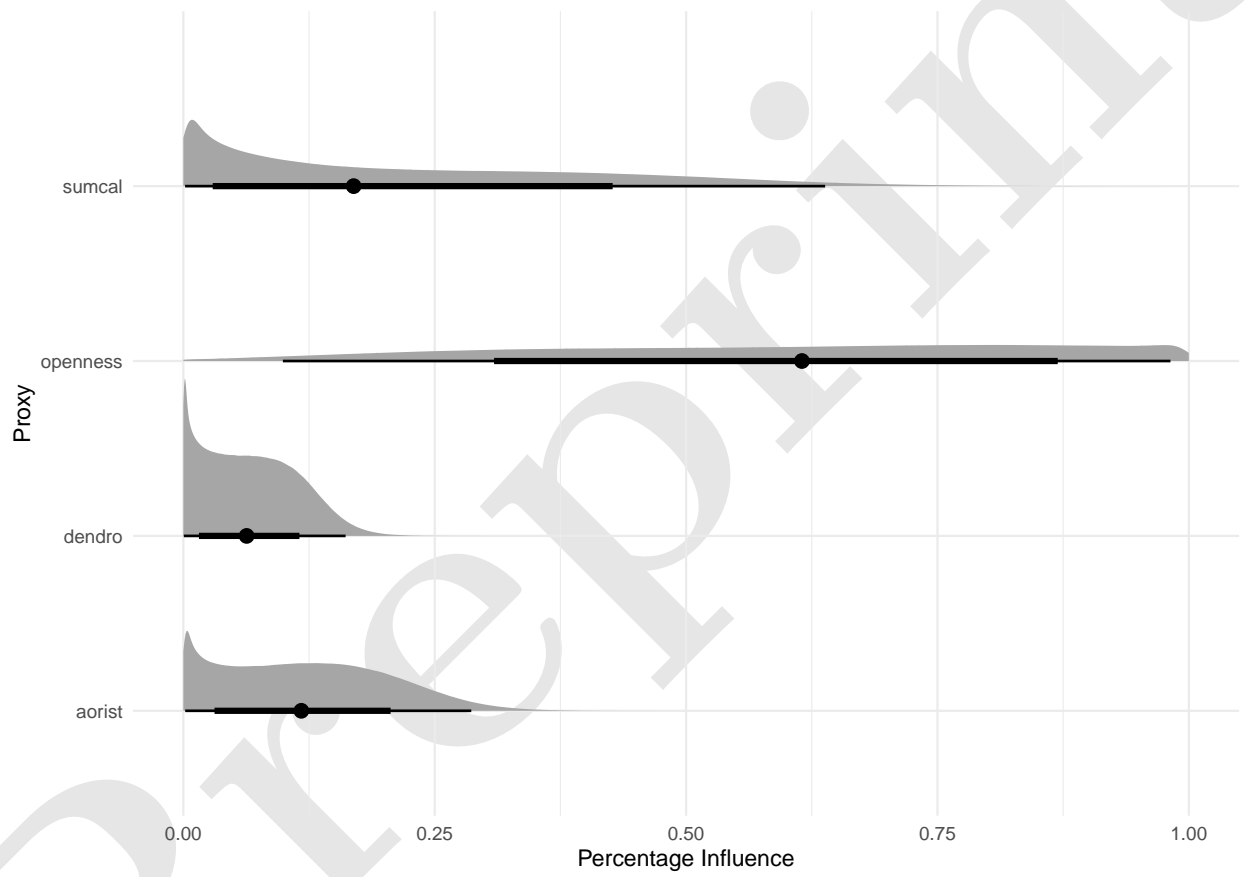


Figure 10: Distribution of influence ratios of proxies on model's final estimation of number of sites.

330 **6. Discussion**

331 **6.1. Reliability of individual proxies**

332 Comparing the model's overall estimate with the individual proxies provides several insights into the quality
333 of these records. The sum calibration, currently the most frequently used proxy for (relative) population
334 change in prehistory, has its large fluctuations damped when considered alongside other proxies. This
335 is especially true of the first fluctuation shortly after 4000 BCE. The expected increase in archaeological
336 remains with the onset of Neolithisation is still clearly visible, but the overall curve is much flatter than
337 the sum calibration itself. The period between 3950 and 3700 BCE, contemporaneous with the first major
338 settlement of the Three Lakes regions' lakeshores, coincides with a noticeable plateau in the calibration curve,
339 producing an overestimation of the ^{14}C density. A second maximum, after 3000 BCE, is supported by the
340 other proxies, and is consequently much more reflected in the overall estimate, coinciding with a smaller and
341 shorter plateau. The rise towards the Middle and Late Bronze Age is also supported by the other proxies,
342 without a significant pattern in the calibration curve. We may conclude that the model is successful in using
343 information from other proxies to sift 'real' fluctuations in the summed radiocarbon record from artefacts of
344 the calibration curve.

345 On average, the model weights the sum calibration at about 20%, significantly less than the 60% afforded
346 to the openness indicator. After an initial increase, which is easily explained by spread of agriculture, the
347 openness indicator tends to fluctuate less and thus has a dampening effect on the overall estimate. In general,
348 this trend in the sum calibration is well reflected in land openness, while changes within the Neolithic and
349 Bronze Age are more gradual.

350 The aoristic sum remains flat over long spans of time. It is not until the Middle and Late Bronze Age that
351 we see a significant rise, which is also apparent in the model's overall estimate. It remains to be seen to
352 what extent modelling of the taphonomic loss (Surovell et al., 2009) could be integrated in this approach.

353 The number of simultaneously existing lakeshore settlements is a temporally and spatially limited estimator,
354 but extremely reliable. Its limitations are reflected in the low overall confidence of the model, since its value
355 is zero over long stretches. However, where it has information potential, such as around and shortly after
356 3800 BCE, 3200 BCE, 1600 BCE or especially around 2750 BCE, its fluctuations have a noticeable influence
357 on the overall estimate. This highlights another potential of our approach: where a proxy has little structure
358 and thus little significance, or where its trends cannot be linked to other indicators, it consequently has little
359 influence. For periods in which it can provide information, however, this will also feed into the overall model,
360 despite a low overall confidence in the estimator.

361 **6.2. Prehistoric population dynamics north of the Swiss Alps**

362 In order to review the reconstruction against the background of established archaeological knowledge, it is
363 useful to overlay conventionally-defined archaeological phase boundaries (Hafner, 2005) on the results of our
364 model (Figure 11).

365 The Early and Middle Neolithic are hardly documented in Switzerland. We must assume a low level of
366 settlement, probably mainly by mobile groups. Isolated Neolithic sites of the LBK and later groups are known
367 in the periphery of Switzerland, but they play a subordinate role (Ebersbach et al., 2012). The evidence
368 of the Neolithic is dense from the so-called Upper Neolithic onwards, connected with the typochronological
369 pottery phases of Egolzwil (late 5th millennium BCE) and Cortaillod respectively Pfyn (first half of the 4th
370 millennium BCE). The first lake shore settlements north of the Alps date to this time too. Here we see a clear
371 increase in the estimated population in the model. In the transition to the Late Neolithic, we know from
372 the lakeshore settlements the so-called Horgen Gap (Hafner, 2005). This is also visible as a slight decrease
373 in the model. In another study (Heitz et al., 2021) we demonstrated that this is in fact probably not a
374 decline in population. Rather communities relocated their settlements to the hinterland of the large lakes in
375 times of stronger lake level rises due to climatic changes. In the Late Neolithic, associated with the Horgen

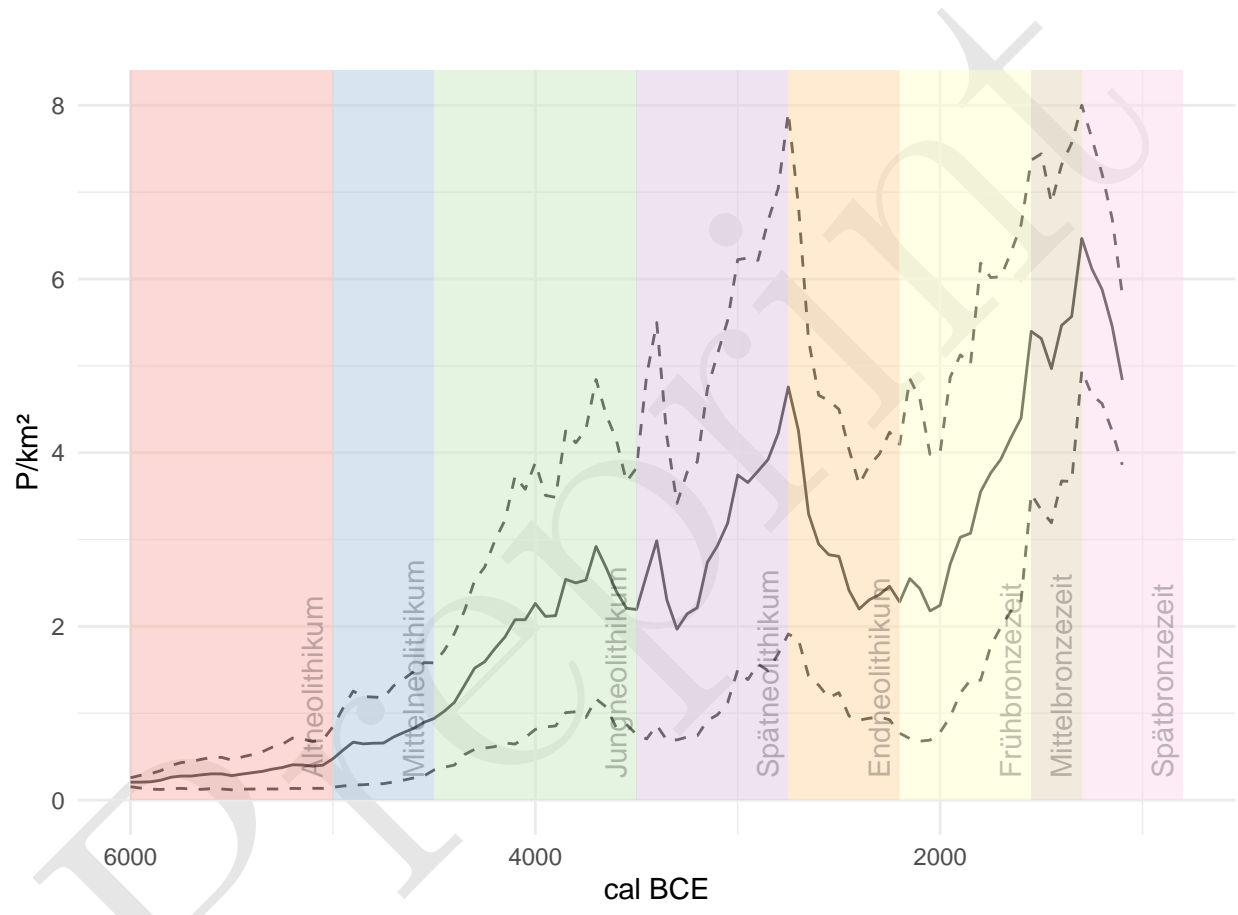


Figure 11: Estimate of population density in relation to the established chronology of the case study area north of the Swiss Alps.

376 pottery, we then see a clear increase in the settlement intensity, which peaks and breaks off at the transition
377 to the Final Neolithic (Hafner, 2004). In the second half of the Early Bronze Age, during which lakeshores
378 were resettled to a smaller extend, there is again a clear increase in population size according to the model,
379 continuing until the Late Bronze Age. The general trends fit very well with the previous reconstructions of
380 population development for Switzerland (see eg. Lechterbeck et al., 2014), while offering higher precision
381 and higher resolution.

382 7. Conclusions

383 The key advance in the model we present is the ability to estimate, in absolute terms, past population
384 sizes and the uncertainty accompanying our present knowledge. These estimates can be a basis for further
385 studies where relative measures of population development are not helpful, such as long-term land use studies.
386 Modelling of large-scale socio-ecological systems based on archaeological data does not have to rely deductive,
387 asynchronous population models (e.g. carrying capacity or ethnographic analogues).

388 We have also demonstrated that, with Bayesian hierarchical modelling, it is possible to achieve a true
389 multi-proxy analysis – as opposed to a juxtaposition of different indicators. This opens up the possibility
390 of quantitatively linking different records and assessing their credibility. We are also able to specifying
391 a confidence interval for the overall estimate. The result is a firmer basis for reconstructing population
392 dynamics and settlement patterns in prehistory.

393 Nevertheless, we consider this model as only the first step towards a more sophisticated Bayesian approach.
394 We have trusted the individual proxies in aggregate, without individualised measurement error. Our esti-
395 mates are based on a limited number of sources, almost all of which are subject to taphonomic biases in the
396 archaeological record. Consequently, we can only transform the model's prediction into an absolute estimate
397 of population density with predefined parameters: settlement size and the initial value of the reconstruction.
398 Overcoming this limitation would represent a major refinement of our approach.

399 Incorporating additional proxies independent of the immediate, time-dependent conditions of the archaeo-
400 logical record could be one way to achieve this. These could be data on settlement sizes, parameters for
401 economic-ecological carrying capacity, demographic data from burial groups or archaeogenetic data on popu-
402 lation sizes. This data is available to varying degrees in different regions. On the Swiss Plateau, for example,
403 we have little data on human remains over large spans of prehistory, in contrast to the abundance of wetland
404 settlements.

405 To apply this approach to other regions, the proxies we use here would have to be adapted to fit local
406 conditions and research histories. By means of large-scale modelling, however, it would be possible to
407 supplement gaps in the data in one region with data from another by regionalisation and a partial transfer
408 of information (partial pooling). Such an extension would be the next logical step in the improvement of
409 the model, to which end we hope to be able to contribute a further study in the near future.

410 8. Acknowledgements

411 Data collection were conducted as part of the project 'Beyond lake settlements' in the doctoral thesis of
412 Julian Laabs, funded by the SNF (project number 152862, PI Albert Hafner) and as part of the XRONOS
413 project, also funded by the SNSF (project number 198153, PI Martin Hinz). The development of the openness
414 index took place within the framework of the project Time and Temporality in Archaeology (project number
415 194326, PI Caroline Heitz), inspired by the cooperation within the project QuantHum (project 169371,
416 PI Marco Conedera), both also funded by the SNSF. Jan Kolář was supported by a long-term research
417 development project (RV67985939) and by a grant from the Czech Science Foundation (19-20970Y). We
418 also thank the Institute of Archaeological Sciences of the University of Bern for its support and faith in
419 the outcome of our modelling project. Finally, we thank (already) the unknown reviewers for their helpful
420 comments, which will certainly improve this manuscript significantly.

⁴²¹ **9. Code availability**

⁴²² The computer code used to generate the Bayesian Population model is provided in full in the Supplementary
⁴²³ Information, together with information about the program and version used. The R code and Data are avail-
⁴²⁴ able online at <https://github.com/MartinHinz/bayesian.demographic.reconstruction.2022> and is archived at
⁴²⁵ <https://doi.org/10.5281/zenodo.6594498>.

426 10. References

- 427 Attenbrow, V., Hiscock, P., 2015. Dates and demography: Are radiometric dates a robust proxy for long-term
428 prehistoric demographic change? *Archaeology in Oceania* 50, 30–36. <https://doi.org/10.1002/arco.5052>
- 429 Auger-Méthé, M., Newman, K., Cole, D., Empacher, F., Gryba, R., King, A.A., Leos-Barajas, V., Mills
430 Flemming, J., Nielsen, A., Petris, G., Thomas, L., 2021. A guide to state-space modeling of ecological
431 time series. *Ecological Monographs* 91, e01470. <https://doi.org/10.1002/ecm.1470>
- 432 Bryant, J., Zhang, J.L., 2018. *Bayesian Demographic Estimation and Forecasting*. Chapman; Hall/CRC.
433 <https://doi.org/10.1201/9780429452987>
- 434 Carleton, W.C., Groucutt, H.S., 2021. Sum things are not what they seem: Problems with point-wise
435 interpretations and quantitative analyses of proxies based on aggregated radiocarbon dates. *The Holocene*
436 31, 630–643. <https://doi.org/10.1177/0959683620981700>
- 437 Childe, V.G. (Ed.), 1936. *Man Makes Himself*. Watts & Co., London.
- 438 Christian Lüthi, 2009. Mittelland (region).
- 439 Crema, E.R., 2022. Statistical Inference of Prehistoric Demography from Frequency Distributions of Radio-
440 carbon Dates: A Review and a Guide for the Perplexed. *Journal of Archaeological Method and Theory*.
441 <https://doi.org/10.1007/s10816-022-09559-5>
- 442 Crema, E.R., Bevan, A., 2021. Inference from large sets of radiocarbon dates: software and methods.
443 *Radiocarbon* 63, 23–39. <https://doi.org/10.1017/RDC.2020.95>
- 444 Crema, E.R., Shoda, S., 2021. A Bayesian approach for fitting and comparing demographic growth models
445 of radiocarbon dates: A case study on the Jomon-Yayoi transition in Kyushu (Japan). *PloS One* 16,
446 e0251695. <https://doi.org/10.1371/journal.pone.0251695>
- 447 David-Elbiali, M., 2000. La Suisse occidentale au IIe millénaire av. J.-C. : Chronologie, culture, intégration
448 européenne. *Cahiers d'archéologie romande*, Lausanne.
- 449 Ebersbach, R., Kühn, M., Stopp, B., Schibler, J., 2012. Die Nutzung neuer Lebensräume in der Schweiz
450 und angrenzenden Gebieten im 5. Jtsd. V. Chr. : Siedlungs- und wirtschaftsarchäologische Aspekte.
451 *Jahrbuch Archäologie Schweiz* 95, 7–34. <https://doi.org/10.5169/SEALS-392483>
- 452 French, J.C., Riris, P., Fernandéz-López de Pablo, J., Lozano, S., Silva, F., 2021. A manifesto for palaeodemography
453 in the twenty-first century. *Philosophical Transactions of the Royal Society B: Biological
454 Sciences* 376, 20190707. <https://doi.org/10.1098/rstb.2019.0707>
- 455 Hafner, A., 2005. Neolithikum: Raum/Zeit-Ordnung und neue Denkmodelle. *Archäologie im Kanton Bern*
456 6B, 431–498.
- 457 Hafner, A., 2004. Vom Spät- zum Endneolithikum. Wandel und Kontinuität um 2700 v. Chr. In Mit-
458 teleuropa. - Vom Endneolithikum zur Frühbronzezeit: Wandel und Kontinuität zwischen 2400 und 1500
459 v.Chr, in: Beier, H.J., Einicke, R. (Eds.), *Varia Neolithica. 3. Beiträge Zur Ur- Und Frühgeschichte
460 Mitteleuropas*. Beier&Beran, Weissbach, pp. 213–249.
- 461 Hafner, A., 1995. Die Frühe Bronzezeit in der Westschweiz. Funde und Befunde aus Siedlungen, Gräbern
462 und Horten der entwickelten Frühbronzezeit. *Staatlicher Lehrmittelverlag Bern* 1995, Bern.
- 463 Hassan, F.A., 1981. *Demographic archaeology, Studies in archaeology*. Academic Press, New York.
- 464 Heitz, C., Hinz, M., Laabs, J., Hafner, A., 2021. Mobility as resilience capacity in northern Alpine Neolithic
465 settlement communities. <https://doi.org/10.17863/CAM.79042>
- 466 Kintigh, K.W., Altschul, J.H., Beaudry, M.C., Drennan, R.D., Kinzig, A.P., Kohler, T.A., Limp, W.F.,
467 Maschner, H.D.G., Michener, W.K., Pauketat, T.R., Peregrine, P., Sabloff, J.A., Wilkinson, T.J., Wright,
468 H.T., Zeder, M.A., 2014. Grand challenges for archaeology. *Proceedings of the National Academy of
469 Sciences* 111, 879–880. <https://doi.org/10.1073/pnas.1324000111>
- 470 Kruschke, J.K., 2015. *Doing Bayesian Data Analysis*. Elsevier. [https://doi.org/10.1016/B978-0-12-405888-0.09999-2](https://doi.org/10.1016/B978-0-12-405888-
471 0.09999-2)
- 472 Laabs, J., 2019. *Populations- und landnutzungsmodellierung der neolithischen und bronzezeitlichen
473 westschweiz (PhD thesis)*. Bern.
- 474 Lechterbeck, J., Edinborough, K., Kerig, T., Fyfe, R., Roberts, N., Shennan, S., 2014. Is Neolithic land
475 use correlated with demography? An evaluation of pollen-derived land cover and radiocarbon-inferred
476 demographic change from Central Europe. *The Holocene* 24, 1297–1307. [https://doi.org/10.1177/0959683614540952](https://doi.org/10.1177/
477 0959683614540952)
- 478 Martínez-Grau, H., Morell-Rovira, B., Antolín, F., 2021. Radiocarbon Dates Associated to Neolithic Con-

- 479 texts (Ca. 5900 – 2000 Cal BC) from the Northwestern Mediterranean Arch to the High Rhine Area.
480 Journal of Open Archaeology Data 9, 1. <https://doi.org/10.5334/joad.72>
- 481 Morris, I., 2013. The measure of civilization: How social development decides the fate of nations. Princeton
482 University Press, Princeton.
- 483 Müller, J., Diachenko, A., 2019. Tracing long-term demographic changes: The issue of spatial scales. PLOS
484 ONE 14, e0208739. <https://doi.org/10.1371/journal.pone.0208739>
- 485 Nikulka, F., 2016. Archäologische Demographie. Methoden, Daten und Bevölkerung der europäischen
486 Bronze- und Eisenzeiten. Sidestone Press, Leiden.
- 487 Price, M.H., Capriles, J.M., Hoggarth, J.A., Bocinsky, R.K., Ebert, C.E., Jones, J.H., 2021. End-to-end
488 Bayesian analysis for summarizing sets of radiocarbon dates. Journal of Archaeological Science 135,
489 105473. <https://doi.org/10.1016/j.jas.2021.105473>
- 490 Ramsey, C.B., 1995. Radiocarbon calibration and analysis of stratigraphy; the OxCal program. Radiocarbon
491 37, 425430.
- 492 Rick, J.W., 1987. Dates as Data: An Examination of the Peruvian Preceramic Radiocarbon Record. American
493 Antiquity 52, 55–73. <https://doi.org/10.2307/281060>
- 494 Riede, F., 2009. Climate and demography in early prehistory: Using calibrated (14)C dates as population
495 proxies. Human Biology 81, 309–337. <https://doi.org/10.3378/027.081.0311>
- 496 Schmidt, I., Hilpert, J., Kretschmer, I., Peters, R., Broich, M., Schiesberg, S., Vogels, O., Wendt, K.P.,
497 Zimmermann, A., Maier, A., 2021. Approaching prehistoric demography: Proxies, scales and scope of
498 the Cologne Protocol in European contexts. Philosophical Transactions of the Royal Society B: Biological
499 Sciences 376, 20190714. <https://doi.org/10.1098/rstb.2019.0714>
- 500 Shennan, S., 2000. Population, Culture History, and the Dynamics of Culture Change. Current Anthropology
501 41, 811–835.
- 502 Shennan, S., Downey, S.S., Timpson, A., Edinborough, K., Colledge, S., Kerig, T., Manning, K., Thomas,
503 M.G., 2013. Regional population collapse followed initial agriculture booms in mid-Holocene Europe.
504 Nature Communications 4, 2486. <https://doi.org/10.1038/ncomms3486>
- 505 Surovell, T.A., Byrd Finley, J., Smith, G.M., Brantingham, P.J., Kelly, R., 2009. Correcting temporal
506 frequency distributions for taphonomic bias. Journal of Archaeological Science 36, 1715–1724. <https://doi.org/10.1016/j.jas.2009.03.029>
- 507 Turchin, P., Brennan, R., Currie, T., Feeney, K., Francois, P., Hoyer, D., Manning, J., Marciniak, A.,
508 Mullins, D., Palmisano, A., Peregrine, P., Turner, E.A.L., Whitehouse, H., 2015. Seshat: The Global
509 History Databank. Cliodynamics 6. <https://doi.org/10.21237/C7clio6127917>
- 510 Zimmermann, A., 2004. Landschaftsarchäologie II. Überlegungen zu prinzipien einer landschaftsarchäologie.

512 11. Author contributions

- 513 • *Martin Hinz*: Conceptualization, Methodology, Software, Validation, Formal analysis, Investigation,
514 Data Curation, Writing - Original Draft, Writing - Review & Editing, Visualization
515 • *Joe Roe*: Software, Validation, Writing - Review & Editing
516 • *Julian Laabs*: Investigation, Data Curation, Writing - Review & Editing
517 • *Caroline Heitz*: Conceptualization, Investigation, Writing - Review & Editing
518 • *Jan Kolář*: Conceptualization, Writing - Review & Editing

519 12. Colophon

520 This report was generated on 2022-11-19 11:53:10 using the following computational environment and de-
521 pendencies:

```
522 #> - Session info -----
523 #>   setting  value
524 #>   version R version 4.2.1 (2022-06-23)
525 #>   os        macOS Big Sur ... 10.16
526 #>   system    x86_64, darwin17.0
527 #>   ui        X11
528 #>   language (EN)
529 #>   collate  en_US.UTF-8
530 #>   ctype    en_US.UTF-8
531 #>   tz       Europe/Zurich
532 #>   date     2022-11-19
533 #>   pandoc   2.19.2 @ /Applications/RStudio.app/Contents/MacOS/quarto/bin/tools/ (via rmarkdown)
534 #>
535 #> - Packages -----
536 #>   package      * version date (UTC) lib source
537 #>   assertthat    0.2.1   2019-03-21 [1] CRAN (R 4.2.0)
538 #>   bitops        1.0-7   2021-04-24 [1] CRAN (R 4.2.0)
539 #>   bookdown      0.30    2022-11-09 [1] CRAN (R 4.2.0)
540 #>   cachem        1.0.6   2021-08-19 [1] CRAN (R 4.2.0)
541 #>   callr         3.7.2   2022-08-22 [1] CRAN (R 4.2.0)
542 #>   class         7.3-20  2022-01-16 [1] CRAN (R 4.2.1)
543 #>   classInt      0.4-8   2022-09-29 [1] CRAN (R 4.2.0)
544 #>   cli            3.4.1   2022-09-23 [1] CRAN (R 4.2.0)
545 #>   colorspace    2.0-3   2022-02-21 [1] CRAN (R 4.2.0)
546 #>   cowplot       * 1.1.1  2020-12-30 [1] CRAN (R 4.2.0)
547 #>   crayon        1.5.2   2022-09-29 [1] CRAN (R 4.2.0)
548 #>   curl           4.3.3   2022-10-06 [1] CRAN (R 4.2.0)
549 #>   DBI            1.1.3   2022-06-18 [1] CRAN (R 4.2.0)
550 #>   devtools       2.4.5   2022-10-11 [1] CRAN (R 4.2.0)
551 #>   digest          0.6.29  2021-12-01 [1] CRAN (R 4.2.0)
552 #>   dplyr          1.0.10  2022-09-01 [1] CRAN (R 4.2.0)
553 #>   e1071          1.7-11  2022-06-07 [1] CRAN (R 4.2.0)
554 #>   ellipsis        0.3.2   2021-04-29 [1] CRAN (R 4.2.0)
555 #>   evaluate        0.17    2022-10-07 [1] CRAN (R 4.2.0)
556 #>   fansi           1.0.3   2022-03-24 [1] CRAN (R 4.2.0)
557 #>   farver          2.1.1   2022-07-06 [1] CRAN (R 4.2.0)
558 #>   fastmap         1.1.0   2021-01-25 [1] CRAN (R 4.2.0)
559 #>   foreign         0.8-82  2022-01-16 [1] CRAN (R 4.2.1)
```

```

560 #> fs 1.5.2 2021-12-08 [1] CRAN (R 4.2.0)
561 #> generics 0.1.3 2022-07-05 [1] CRAN (R 4.2.0)
562 #> ggmap * 3.0.0 2019-02-05 [1] CRAN (R 4.2.0)
563 #> ggplot2 * 3.3.6 2022-05-03 [1] CRAN (R 4.2.0)
564 #> ggrepel * 0.9.1 2021-01-15 [1] CRAN (R 4.2.0)
565 #> ggsn * 0.5.0 2019-02-18 [1] CRAN (R 4.2.0)
566 #> glue 1.6.2 2022-02-24 [1] CRAN (R 4.2.0)
567 #> gtable 0.3.1 2022-09-01 [1] CRAN (R 4.2.0)
568 #> here * 1.0.1 2020-12-13 [1] CRAN (R 4.2.0)
569 #> highr 0.9 2021-04-16 [1] CRAN (R 4.2.0)
570 #> htmltools 0.5.3 2022-07-18 [1] CRAN (R 4.2.0)
571 #> htmlwidgets 1.5.4 2021-09-08 [1] CRAN (R 4.2.0)
572 #> httpuv 1.6.6 2022-09-08 [1] CRAN (R 4.2.0)
573 #> httr 1.4.4 2022-08-17 [1] CRAN (R 4.2.0)
574 #> jpeg 0.1-9 2021-07-24 [1] CRAN (R 4.2.0)
575 #> KernSmooth 2.23-20 2021-05-03 [1] CRAN (R 4.2.1)
576 #> knitr 1.40 2022-08-24 [1] CRAN (R 4.2.0)
577 #> labeling 0.4.2 2020-10-20 [1] CRAN (R 4.2.0)
578 #> later 1.3.0 2021-08-18 [1] CRAN (R 4.2.0)
579 #> lattice 0.20-45 2021-09-22 [1] CRAN (R 4.2.1)
580 #> lifecycle 1.0.3 2022-10-07 [1] CRAN (R 4.2.0)
581 #> magrittr 2.0.3 2022-03-30 [1] CRAN (R 4.2.0)
582 #> maptools 1.1-5 2022-10-21 [1] CRAN (R 4.2.0)
583 #> memoise 2.0.1 2021-11-26 [1] CRAN (R 4.2.0)
584 #> mime 0.12 2021-09-28 [1] CRAN (R 4.2.0)
585 #> miniUI 0.1.1.1 2018-05-18 [1] CRAN (R 4.2.0)
586 #> munsell 0.5.0 2018-06-12 [1] CRAN (R 4.2.0)
587 #> pillar 1.8.1 2022-08-19 [1] CRAN (R 4.2.0)
588 #> pkgbuild 1.3.1 2021-12-20 [1] CRAN (R 4.2.0)
589 #> pkgconfig 2.0.3 2019-09-22 [1] CRAN (R 4.2.0)
590 #> pkgload 1.3.0 2022-06-27 [1] CRAN (R 4.2.0)
591 #> plyr 1.8.7 2022-03-24 [1] CRAN (R 4.2.0)
592 #> png 0.1-7 2013-12-03 [1] CRAN (R 4.2.0)
593 #> prettyunits 1.1.1 2020-01-24 [1] CRAN (R 4.2.0)
594 #> processx 3.7.0 2022-07-07 [1] CRAN (R 4.2.0)
595 #> profvis 0.3.7 2020-11-02 [1] CRAN (R 4.2.0)
596 #> promises 1.2.0.1 2021-02-11 [1] CRAN (R 4.2.0)
597 #> proxy 0.4-27 2022-06-09 [1] CRAN (R 4.2.0)
598 #> ps 1.7.1 2022-06-18 [1] CRAN (R 4.2.0)
599 #> purrr 0.3.5 2022-10-06 [1] CRAN (R 4.2.0)
600 #> R6 2.5.1 2021-08-19 [1] CRAN (R 4.2.0)
601 #> RColorBrewer 1.1-3 2022-04-03 [1] CRAN (R 4.2.0)
602 #> Rcpp 1.0.9 2022-07-08 [1] CRAN (R 4.2.0)
603 #> remotes 2.4.2 2021-11-30 [1] CRAN (R 4.2.0)
604 #> rgdal 1.6-2 2022-11-09 [1] CRAN (R 4.2.0)
605 #> RgoogleMaps 1.4.5.3 2020-02-12 [1] CRAN (R 4.2.0)
606 #> rjson 0.2.21 2022-01-09 [1] CRAN (R 4.2.0)
607 #> rlang 1.0.6 2022-09-24 [1] CRAN (R 4.2.0)
608 #> rmarkdown 2.17 2022-10-07 [1] CRAN (R 4.2.0)
609 #> rnaturalearth * 0.1.0 2017-03-21 [1] CRAN (R 4.2.0)
610 #> rprojroot 2.0.3 2022-04-02 [1] CRAN (R 4.2.0)
611 #> rstudioapi 0.14 2022-08-22 [1] CRAN (R 4.2.0)
612 #> s2 1.1.0 2022-07-18 [1] CRAN (R 4.2.0)
613 #> scales 1.2.1 2022-08-20 [1] CRAN (R 4.2.0)

```

```
614 #> sessioninfo      1.2.2  2021-12-06 [1] CRAN (R 4.2.0)
615 #> sf                * 1.0-8  2022-07-14 [1] CRAN (R 4.2.0)
616 #> shiny              1.7.3  2022-10-25 [1] CRAN (R 4.2.0)
617 #> sp                * 1.5-0  2022-06-05 [1] CRAN (R 4.2.0)
618 #> stringi             1.7.8  2022-07-11 [1] CRAN (R 4.2.0)
619 #> stringr             1.4.1  2022-08-20 [1] CRAN (R 4.2.0)
620 #> tibble              3.1.8  2022-07-22 [1] CRAN (R 4.2.0)
621 #> tidyverse            1.2.1  2022-09-08 [1] CRAN (R 4.2.0)
622 #> tidyselect           1.2.0  2022-10-10 [1] CRAN (R 4.2.0)
623 #> units               0.8-0  2022-02-05 [1] CRAN (R 4.2.0)
624 #> urlchecker          1.0.1  2021-11-30 [1] CRAN (R 4.2.0)
625 #> usethis              2.1.6  2022-05-25 [1] CRAN (R 4.2.0)
626 #> utf8                1.2.2  2021-07-24 [1] CRAN (R 4.2.0)
627 #> vctrs               0.4.2  2022-09-29 [1] CRAN (R 4.2.0)
628 #> withr               2.5.0  2022-03-03 [1] CRAN (R 4.2.0)
629 #> wk                  0.7.0  2022-10-13 [1] CRAN (R 4.2.0)
630 #> xfun                 0.33   2022-09-12 [1] CRAN (R 4.2.0)
631 #> xtable              1.8-4  2019-04-21 [1] CRAN (R 4.2.0)
632 #> yaml                 2.3.5  2022-02-21 [1] CRAN (R 4.2.0)
633 #>
634 #> [1] /Library/Frameworks/R.framework/Versions/4.2/Resources/library
635 #>
636 #> -----
```